

A Critical Epithelial Survival Axis Regulated by MCL-1 Maintains Thymic Function in Mice

Reema Jain^{1,2}, Julie M. Sheridan^{1,2}, Antonia Policheni^{1,2}, Melanie Heinlein^{1,2}, Luke C. Gandolfo^{1,3}, Grant Dewson^{1,2}, Gordon K Smyth^{1,3}, Stephen N. Sansom⁴, Nai Yang Fu^{5,6}, Jane E. Visvader^{1,2}, Georg A. Holländer⁷, Andreas Strasser^{1,2}, Daniel H.D. Gray^{1,2}

¹Walter and Eliza Hall Institute of Medical Research, Melbourne, VIC, Australia;

²Department of Medical Biology, University of Melbourne, Melbourne, VIC, Australia; ³ School of Mathematics & Statistics, University of Melbourne, Melbourne, VIC, Australia; ⁴ Kennedy Institute of Rheumatology, University of Oxford, UK; ⁵

Programme in Cancer & Stem Cell Biology, Duke-NUS Medical School, Singapore;

⁶Biology Department, College of Science, Shantou University, Shantou 515063, China

⁷Weatherall Institute for Molecular Medicine, University of Oxford, UK

Correspondence to: dgray@wehi.edu.au

T: +61 3 9345 2741

F: +61 3 9347 0852

Text count: 3976

Abstract count: 185

Figure count: 7 figures, 6 supplementary figures

Reference count: 59

Short Title: MCL-1 regulates thymic epithelial cell survival

Key Points:

1. MCL-1 is essential, but BCL-2 and BCL-XL are dispensable, for thymic epithelial cell survival and thymic function
2. EGF upregulates MCL-1 in TECs

Abstract

T cell differentiation is governed by interactions with thymic epithelial cells (TECs) and defects in this process undermine immune function and tolerance. To uncover new strategies to restore thymic function and adaptive immunity in immunodeficiency, we sought to determine the molecular mechanisms that control life and death decisions in TEC. Guided by gene expression profiling, we created mouse models which specifically deleted pro-survival genes in TEC. We found that while BCL-2 and BCL-XL were dispensable for TEC homeostasis, MCL-1 deficiency impacted on TEC as early as E15.5, resulting in early thymic atrophy and T cell lymphopenia, with near complete loss of thymic tissue by 2 months of age. MCL-1 was not necessary for TEC differentiation but was continually required for the survival of mature cortical and medullary TEC, and the maintenance of thymic architecture. A screen of TEC trophic factors in organ cultures showed that epidermal growth factor (EGF) upregulated MCL-1 via MAPK/ERK kinase activity, providing a molecular mechanism for the support of TEC survival. This signalling axis governing TEC survival and thymic function represents a new target for strategies for thymic protection and regeneration.

Introduction

TECs are an integral part of the thymic microenvironment and are essential for all major steps in thymocyte differentiation. The cortical epithelium drives commitment of haematopoietic precursors to the T cell lineage, their proliferation and the positive selection of thymocytes with potentially useful TCRs¹. Medullary TECs (mTEC) are essential for negative selection and regulatory T (Treg) cell development, in part due to their expression of the autoimmune regulator, AIRE². Numerous studies have revealed that defects in TEC differentiation can, in turn, perturb T cell differentiation to cause immunodeficiency or autoimmune disease³. Given the importance of TECs for acquired immunity, the molecular mechanisms that govern their generation and function have been a major focus in the field, with a view to developing strategies to improve or restore thymic function in immunocompromised patients^{4,5}. These mechanisms are likely to be highly dynamic. The TEC compartment exhibits a high rate of proliferation and is capable of replacement within approximately 2 weeks in the adult mouse⁶⁻⁸. Distinct TEC subsets exhibit differential mitotic rates, a feature that supports the concept that adult TEC homeostasis is maintained by continual proliferation and differentiation of progenitor cells counterbalanced by cell attrition.

TEC in adult mice can be divided into four major populations based on location, phenotype and function: cortical TEC (cTEC), medullary TEC that express low levels of MHC II/CD80 (mTEC^{low}), mTEC that express high levels of MHC II/CD80 that can be divided into AIRE⁺ mTEC^{high}, and AIRE⁻ mTEC^{high}. The mTEC^{low} subset has a low proliferative rate and includes at least some progenitors of mTEC^{high}⁷⁻¹⁰. The greatest levels of proliferation have been observed in mTEC^{high}, particularly in the AIRE⁻ subset⁷⁻⁹. It is currently unclear how TECs are lost and few

studies have considered the mechanisms controlling attrition. AIRE expression can lead to heightened apoptosis *in vitro*^{8,11,12}; however, fate-mapping studies indicate that at least some TEC survive AIRE expression *in vivo* and downregulate this transcriptional regulator^{13,14}. Therefore, while we can infer the rate of TEC loss required to counterbalance their high rate of proliferation; the mechanisms, sequence and contribution of TEC death to thymic function remain unknown.

The intrinsic pathway of apoptosis (also called the mitochondrial, stress-induced or BCL-2 regulated pathway) is necessary for embryogenesis, deletion of auto-reactive lymphocytes and tissue homeostasis¹⁵. Disruption of the mitochondrial outer membrane represents the “point-of-no-return” in the intrinsic pathway of apoptosis and is strictly regulated via interactions among over 20 members of the BCL-2 family of proteins. These proteins can be divided into three functional factions: 1) the pro-apoptotic BH3-only proteins, 2) the pro-survival proteins and, 3) the effector proteins, BAX and BAK (and perhaps BOK)¹⁵. In healthy cells, the pro-survival proteins BCL-2, BCL-XL, MCL-1, BCL-W and BFL-1/A1 prevent BAX and BAK activation and apoptosis. However, cytotoxic stressors can upregulate or activate pro-apoptotic BH3-only proteins (BIM, PUMA, NOXA, BID, BAD, BIK, HRK and BMF), which sequester pro-survival proteins and/or directly activate BAX and BAK to trigger apoptosis. Different cell types respond to cytotoxic stimuli with varying sensitivity because the expression and regulation of the BCL-2 family of proteins differ greatly¹⁵. This variation precludes the prediction of how cells will respond to stress but also creates opportunities for tissue-specific targeting of survival and death proteins for therapeutic benefit^{16,17}. In this study, we aimed to understand the molecular pathways that control TEC survival and thymic function. Surprisingly, we found that BCL-2 and BCL-XL were dispensable for TEC survival; however,

MCL-1 was essential for the maintenance of specific TEC subsets. We found that EGF is a positive regulator of this pro-survival protein in TEC, identifying MCL-1 as a tractable target for the amelioration of age- or damage-induced thymic atrophy.

Methods

Mice

Mcl1^{lox/lox18}, *Bclx_L*^{lox/lox19}, *Bcl2*^{lox/lox20} mice, *Rosa*^{CreERT2}*Mcl1*^{lox/lox21}, *Foxn1*^{Cre22}, *Bak*^{-/-23}, *Bax*^{lox/lox24}, *Aire*^{GFP/+} and *Aire*^{-/-25} mice were either generated and maintained on a C57BL/6 background or had been generated on a mixed 129/C57BL/6 background and then backcrossed at least 10 times to C57BL/6 background (except mice which were backcrossed 6 times). The *Mcl1*^{ΔK5} mice were on a mixed FVB/C57BL/6 background²⁶. The *Foxn1*^{Cre/+}*Mcl1*^{lox/-} mice were generated by crossing *Mcl1*^{+/-} males²¹ with *Mcl1*^{ΔFoxn1} or *Foxn1*^{Cre/+}*Mcl1*^{lox/+} females.

All mice were raised under specific pathogen-free housing conditions according to the regulations of the Walter and Eliza Hall Institute of Medical Research, the Swiss Federal Government and the Weatherall Institute of Molecular Medicine. All animal experiments comprised of 3 or more mice (unless otherwise stated) in both control and experimental groups and included age-matched controls.

Thymus digestion

Thymi were digested individually as previously described²⁷. Briefly, connective tissue was removed and the two thymic lobes separated. Several snips were made in each lobe with surgical scissors and the fragments agitated in 5 mL of RPMI-1640 with 25.96 mM HEPES with a wide-bore pipette tip. The supernatant was replaced by 1 mL of digestion buffer (RPMI-HEPES supplemented with Liberase TM (Roche) at 0.5 Wunsch units (U) per mL and DNase I at 0.1% (w/v) (Sigma-Aldrich) and thymic tissue was then digested at 37°C for 15 min with gentle agitation every 5 min. At the end of the first digestion, the supernatant was recovered and replaced with 500μL of digestion buffer. Digestion was repeated for 15 min at 37°C with gentle agitation after every 5 min.

Antibodies and flow cytometry

Surface staining of TEC was performed using the following antibodies that were made at The Walter and Eliza Hall Institute, unless otherwise stated. Anti-mouse CD16/32 FcR-block (clone 2.4G2), anti-mouse CD45 PerCP/Cy5.5 (clone 30-F11, Biolegend), anti-mouse CD31 PerCP/Cy5.5 (clone 390, Biolegend), anti-mouse Ter119 PerCP/Cy5.5 (clone TER119, Biolegend), anti-mouse CD326 (EPCAM) APC/Cy7 (clone G8.8, Biolegend), anti-mouse H-2K^b Pacific Blue (Clone AF6-88.5, Biolegend), anti-H2-A/E FITC or APC (clone M5/114.15.2), anti-H2-A/E BV421 (clone M5/114.15.2, Biolegend), biotinylated UEA-1 lectin (Vector labs, USA), anti-mouse Ly51 PE or FITC (clone 6C3, Biolegend), biotinylated anti-mouse CD40 (clone FGK45.5), CD80 BV421 (clone 16-10A1, Biolegend) and anti-human CD4 PE (clone OKT4). Second step staining with streptavidin PE/Cy7 (BD Biosciences, USA) was used to detect biotinylated UEA1 (Vector Laboratories). Propidium iodide (PI) or DAPI at a final concentration of 2.5 µg/mL was added to samples just prior to data acquisition to label dead cells. Intracellular staining with anti-human Ki67 FITC (clone MOPC-21, BD Pharmingen), anti-mouse AIRE FITC (clone 5H12), anti-mouse β5t (MBL), anti-mouse BCL-2 PE (clone BCL/10C4, Biolegend), anti-mouse BCL-XL (clone E18, Abcam) and anti-mouse MCL-1 Alexa 647 (clone AA3²⁸) was performed after fixation and permeabilization with the eBioscience FoxP3 kit.

Lymphocytes were stained using the following antibodies: anti-mouse CD4 APC (clone H129), anti-mouse CD4 PerCP/Cy5.5 (GK1.5, Biolegend), anti-mouse TCRβ PE/Cy7 (H57.59.1, Biolegend), anti-mouse CD8 APC/Cy7 or BV650 (clone 53-6.7, Biolegend), anti-mouse CD25 PE or BV510 (clone PC61, Biolegend), anti-mouse CD44 PE or FITC (clone IM781), anti-mouse CD62L APC/Cy7 (clone MEL-14, Biolegend). The immature thymocyte depletion cocktail contained biotinylated

antibodies against mouse NK1.1 (clone PK136, Biolegend), TER119 (TER119), GR1 (clone RB6-8C5), Mac-1 (clone M1-170) and B220 (RA3-6B2). Second step labelling with streptavidin BV786 (Biolegend) was used to detect the biotinylated antibodies. Screening of TCRV β repertoire in the CD4⁺ and CD8⁺ populations were analysed using the Mouse V β TCR Screening Panel (BD Pharmingen) antibodies. Intracellular staining using anti-mouse FOXP3 eFluor-450 (clone FJK-165, eBioscience) was performed after fixation and permeabilisation with eBioscience FOXP3 kit. Samples were either acquired, enriched or sorted using a Fortessa X20 analyser (BD Biosciences), LSR II (BD Bioscience) AutoMACS (Miltenyi Biotec) and Moflo Legacy (Beckon Coulter). FACS data were analysed using FlowJo software 9.9 (TreeStar).

Immunohistology

Adult (2 month-old) and neonatal (day 9) thymi were isolated, embedded in Tissue-Tek O.C.T compound (Sakura Finetek, U.S.A.) and snap frozen in a liquid nitrogen/isopentane slurry. Sections of 5-8 μ m were cut using a Microm HM550 Cryostat (Thermo Scientific). Sections were air-dried for 20 min and stored at -80°C prior to staining. Sections were blocked with 5% (v/v) goat serum in PBS with 0.5% Tween-20 (v/v) for 30 min at room temperature before incubation with primary antibodies for 30 minutes. Primary antibodies included biotinylated anti-mouse pan-keratin (LifeSpan BioSciences, clone Lu-5), anti-mouse K5 (Covance, clone Poly 19055), biotinylated UEA-1 lectin (Vector labs, USA), anti-mouse DEC205-FITC (clone NLDC145) and anti-mouse AIRE-Alexa647 (clone 5H12), anti-mouse K8 (clone Troma-I, DSHB) and ER-TR7 (provided by Prof Richard Boyd, Monash University). Following three washes in PBS, 5 min each, sections were then incubated with appropriate secondary antibody (anti-rabbit Ig Alexa-555 (Life Technologies))

and streptavidin FITC (Invitrogen) for 30 min, counterstained with DAPI (Sigma-Aldrich), then mounted with Vectashield (Vector labs). Images were collected using a LSM780 confocal with Zen 2012 SP2 (black) software v11.0 (Zeiss). Single optical sections and maximal intensity projection images were processed for presentation using OMERO²⁹.

Renal capsule grafting of *Rosa*^{CreERT2}*Mcl1*^{lox/lox} fetal thymus

Thymic lobes were dissected from E15.5 embryos and cultured for 2 days in FTOC medium (see FTOC). One lobe from control (*Rosa*^{CreERT2}*Mcl1*^{+/+} or *Rosa*^{+/+}*Mcl1*^{lox/lox}) and one lobe from experimental (*Rosa*^{CreERT2}*Mcl1*^{lox/lox}) were transplanted under the renal capsule of the recipient C57BL/6 Ly5.1 males at the anterior and posterior poles of the kidney, respectively. Grafts were allowed to reconstitute for 4-8wks, then mice were orally gavaged with 200 mg tamoxifen/kg (Sigma-Aldrich) in peanut oil/10% ethanol for three alternate days and were then analysed at 2 months, 1 month or 5 days after the third dose.

Data analysis

Statistical analyses were performed using Prism version 6. Outliers were not excluded in any of the experiments. Experiments containing three or more groups were analysed using ANOVA followed by a Tukey's post-hoc test. Experiments with two groups were analysed with two-tailed Student's t-test. P-values <0.05 were considered as the threshold for statistical significance for all statistical tests. RNA-sequencing (Figure 1A) reads from (GEO accession GSE53110)²⁵ were re-mapped with Hisat2³⁰ against the mouse genome (mm10) before quantitation of Ensembl 83 genes with Cufflinks³¹. Inter-sample normalisation was performed with the upper quartile method based on house-keeping gene³² expression.

Results

Differential expression and requirement for BCL-2 family members among TEC subsets

To determine the transcriptional profiles of BCL-2 family genes in TECs, we analysed RNA sequence data from TEC subsets²⁵. We found that *Bcl2*, *Bcl2l1* (encoding BCL-XL; hereafter referred to as *Bclx_L*) and *Mcl1* were differentially expressed among the major TEC subsets (**Figure 1A**), with evidence of high co-expression of *Bclx_L* and *Mcl1* in mTEC populations. These data were supported by intracellular flow cytometric analysis that revealed similar levels of BCL-2 throughout TEC subsets and the highest levels of BCL-XL and MCL-1 in mTEC^{hi} (**Figure 1B**). In order to investigate the functional importance of these proteins during TEC development and homeostasis, we deleted these genes only in TEC by crossing *Foxn1*^{Cre} transgenic mice²² with mice bearing *loxP* flanked *Bcl2*²⁰, *Bclx_L*¹⁹ or *Mcl1*¹⁸. Efficient and early TEC-specific deletion of these pro-survival genes was confirmed by flow cytometry and Western blotting, with at least 90% of TECs deleting the respective genes as early as E13.5 (**Figure 1C and supplementary Figures S1A-C**).

TEC-specific deletion of *Bclx_L* (*Bclx_L*^{ΔFoxn1}) or *Bcl2* (*Bcl2*^{ΔFoxn1}) did not cause gross thymic abnormalities in 2 month-old adult mice (**Figure 1D, E**). By contrast, TEC-specific loss of *Mcl1* (*Mcl1*^{ΔFoxn1}) induced marked thymic hypoplasia in adult mice (**Figure 1D, E**). Analysis of thymic ontogeny in *Mcl1*^{ΔFoxn1} mice revealed decreased thymic cellularity as early as E15.5 compared to controls (**Figure 1F**). This defect worsened with age, such that 2 month-old mice exhibited approximately 20-fold lower thymic cellularity compared to controls (**Figure 1F**). These data show that MCL-1 expression by TEC is essential for normal thymic development and homeostasis.

Impaired thymocyte differentiation and T cell lymphopenia in *Mcl1*^{ΔFoxn1} mice

To test the function of the hypotrophic thymi in *Mcl1*^{ΔFoxn1} mice, we analysed thymocyte differentiation in young (day 9) and adult (2 month-old) *Mcl1*^{ΔFoxn1} mice. Populations of CD4⁻CD8⁻ double negative (DN), CD4⁺CD8⁺ double positive (DP), CD4⁺CD8⁻ and CD4⁻CD8⁺ single positive (SP) thymocytes were present, indicating some level of T cell differentiation in *Mcl1*^{ΔFoxn1} mice (**Figure 2A and supplemental Figure S2A**). However, there was a major numerical deficit in all thymocyte subsets from *Mcl1*^{ΔFoxn1} mice, particularly DP (**Figure 2A**). Analysis of the different subsets of immature DN progenitors (DN1, CD25⁻CD44⁺; DN2, CD25⁺CD44⁺; DN3, CD25⁺CD44⁻; DN4, CD25⁻CD44⁻) revealed that all four subsets were reduced, with some indication of a partial block in DN3 thymocytes in 2 month-old *Mcl1*^{ΔFoxn1} mice (**Figure 2A, supplemental Figure S2B**). Studies have shown that the number of DP cells is proportional to the number of DN cells in the thymus^{33,34}. Therefore, a decrease in DP numbers in *Mcl1*^{ΔFoxn1} mice could be a result of the decrease in the number of DN cells or the import of progenitors. Likewise, a decline in the numbers of critical FOXP3⁺ regulatory T (Treg) cells that depend upon the medullary microenvironment for their development was observed³⁵ (**Figure 2B**).

Consistent with the observed thymocyte deficiency, *Mcl1*^{ΔFoxn1} mice had a paucity of peripheral T cells (**Figures 3A and supplemental Figure S3A**). Although peripheral B cell numbers were nearly normal, both CD4⁺ and CD8⁺ T cells were reduced in day 9 and 2 month-old *Mcl1*^{ΔFoxn1} mice (**Figure 3A and supplemental Figure S3A, B**). This T cell lymphopenia was most pronounced in the naïve CD44^{low}CD62L^{high} compartment that relies upon thymic output³⁶ (**Figures 3B, C and supplemental Figure S3C**). Conversely, there was a proportional expansion of T cells with a central/effector memory, regulatory or proliferating (Ki67⁺) phenotype

observed in young and old *MclI* ^{Δ Foxn1} mice (**Figures 3B-E and supplemental Figure S3C-E**), with evidence of an altered TCR repertoire (**supplemental Figure S3F**). This outcome likely reflects lymphopenia-induced T cell expansion in the periphery in response to the deficit in T cell production by the thymus, with a consequent increase in the bioavailability of homeostatic cytokines, such as IL-2 and IL-7. Interestingly, these features, along with lower numbers of Tregs and medullary hypoplasia in neonates, did not result in autoimmunity; we could not detect signs of excessive leukocyte infiltration into tissues of aged *MclI* ^{Δ Foxn1} mice (data not shown).

To address whether the residual thymic tissue observed in *MclI* ^{Δ Foxn1} mice was due to incomplete deletion of all *MclI* alleles, we analysed adult *Foxn1*^{cre/+} *MclI*^{lox/-} mice. These mice also exhibited severe thymic atrophy and T cell lymphopenia to a similar extent to *MclI* ^{Δ Foxn1} mice, with some residual thymopoiesis (**supplemental Figure S4 and data not shown**). Together, these data indicate that the thymic defects in *MclI* ^{Δ Foxn1} mice cause substantial distortion of the peripheral T cell pool.

MCL-1 is essential for TEC homeostasis

To determine how the loss of MCL-1 in TEC impaired thymic function in *MclI* ^{Δ Foxn1} mice, we carried out a detailed analysis of CD45⁻EpCAM⁺MHC II⁺ TEC at key time points (*MclI*-deficiency did not reduce MHC II levels on TEC, data not shown). Flow cytometric analysis revealed that MCL-1 deficiency reduced TEC numbers as early as E15.5 and that this defect was exacerbated with age (**Figure 4A**). Nevertheless, all major TEC subsets could be recovered from day 9 *MclI* ^{Δ Foxn1}, including cTEC, mTEC^{low}, AIRE⁻ mTEC^{high} and AIRE⁺ mTEC^{high} (**Figure 4B-F**). However, there was a severe deficiency in mTEC number in day 9 and 2 month-old *MclI* ^{Δ Foxn1} mice that affected both phenotypically immature (CD80⁻/MHC II^{low}) and

mature (CD80⁺/MHC II^{high}) mTEC, including the AIRE⁺ mTEC^{high} subset that is critical for imposing immune tolerance (**Figure 4B-F**)^{8,10}. The proportion of proliferating TEC (Ki67⁺) was higher in E15.5 and day 9 *Mcl1*^{ΔFoxn1} mice (**Figure 4G, H**), suggesting that either there is a specific loss of non-dividing TECs or the remaining population undergoes heightened proliferation to compensate for TEC death caused by the loss of MCL-1. Regardless, these data indicate that MCL-1 is not critical for the differentiation of the major TEC subpopulations, but is essential for their maintenance.

TEC-specific MCL-1-deficiency also impacted upon the overall thymic architecture. Immunohistological analysis of the thymus from *Mcl1*^{ΔFoxn1} mice revealed extensive and progressive disruption of cortical (labelled with anti-keratin-8, anti-DEC205) and medullary regions (labelled with anti-keratin-5 and UEA-1) (**Figures 4I, J, supplemental Figure 5A, B**). The few small medullary areas containing AIRE⁺ TECs in *Mcl1*^{ΔFoxn1} mice at day 9 were nearly completely absent by 2 months of age (**Figure 4K, data not shown**) and thymi were heavily populated by ER-TR7⁺ thymic fibroblasts (**Figure 4L**). These data show that TEC-specific MCL-1-deficiency induces near complete loss of mTEC in adult mice, cTEC compositional changes and the disruption of the entire thymic microenvironment.

Although the cTEC numbers in *Mcl1*^{ΔFoxn1} mice were comparable to controls, the early thymocyte defects prompted a deeper analysis of the functional competence of this subset. A multi-dimensional scaling plot of RNA sequencing data from FACS purified TEC subsets from 1 month-old *Mcl1*^{ΔFoxn1} and control mice revealed grossly altered gene expression in cTEC, but not mTEC (**Figure 5A and data not shown**). In particular, the cTEC population in *Mcl1*^{ΔFoxn1} mice displayed differential expression of TEC progenitor genes (e.g. increased *Foxn1*, *Psb11* (aka beta5t), reduced *Plet1*,

Cldn3, *Cldn4*) and mediators of early thymocyte differentiation (e.g. reduced *Il7*, *Ccl19*, *Ccl21*, increased *Dll4*), suggesting compositional changes in the absence of MCL-1 that impact on mature cTEC function (**Figure 5B**). These findings were supported by flow cytometric analysis of $\beta 5t$, CD40 and MHC I, CD80 on cTEC and TEC, respectively, from *Mcl1* ^{Δ Foxn1} mice (**Figure 5C-F**).

To test whether MCL-1 was required to antagonise the intrinsic pathway of apoptosis in TEC, we also deleted the key effector proteins BAK and/or BAX in *Mcl1* ^{Δ Foxn1} mice. Compound deletion of these genes (or loss of BAK alone) was sufficient to completely rescue thymic atrophy, TEC numbers, composition and thymus function in *Mcl1* ^{Δ Foxn1} mice, indicating that MCL-1 is essential to prevent excessive TEC apoptosis (**Figure 5G, H and data not shown**).

To verify the requirement for MCL-1 in TEC survival and homeostasis, we used an alternative epithelial-specific Cre transgenic mouse. All TECs express K5 early during development³⁷, so we employed a previously published *K5*^{Cre} strain³⁸ to delete *Mcl1* and found that young *Mcl1* ^{Δ K5} mice exhibited thymic atrophy similar to that observed in the *Mcl1* ^{Δ Foxn1} mice (**Supplemental Figure 6A, B**). The low numbers of TEC that remained in *Mcl1* ^{Δ K5} mice supported residual thymic function and a diminished peripheral T cell compartment (**Supplemental Figure 6C, D, E**). Collectively, these data identify an essential role for MCL-1 in maintaining the mature TEC compartment throughout thymus development.

Ongoing requirement for MCL-1 in TEC survival

Is the thymic atrophy in adult *Mcl1* ^{Δ Foxn1} and *Mcl1* ^{Δ K5} mice caused by the loss of TEC progenitors during development, or is it due to an ongoing requirement for this pro-survival protein for steady-state TEC homeostasis? To address this question,

we turned to an inducible deletion system, where ablation of *Mcl1* could be achieved specifically in the thymic stroma after the microenvironment had been fully established. Thymic lobes from E15.5 *Rosa^{CreERT2}Mcl1^{lox/lox}* embryos were grafted under the renal capsule of C57BL/6-Ly5.1 mice (control lobes without either *Rosa^{CreERT2}* or *loxP* flanked *Mcl1* alleles or heterozygotes were placed on the opposite pole of the kidney). Host haematopoietic cells were allowed to reconstitute between 4-8 weeks, then Cre-ERT2-mediated deletion of *Mcl1* was induced by tamoxifen administration (**Figure 6A**). We found that thymic grafts from *Rosa^{CreERT2}Mcl1^{lox/lox}* lobes could be recovered 5 days following tamoxifen treatment but that substantial loss of TEC had already occurred following deletion of MCL-1 (**Figure 6B-D**). This loss of TEC apparently induced thymic atrophy because only residual thymic tissue could be recovered from *Rosa^{CreERT2}Mcl1^{lox/lox}* grafts two months after treatment, while control lobes remained intact (**Figure 6B, C**). Although the deletion of MCL-1 was not limited to TECs in this model, the extent and kinetics of thymic atrophy observed in this grafting and acute deletion system recapitulated that observed in adult *Mcl1^{ΔFoxn1}* mice, supporting the notion that there is an ongoing requirement for MCL-1 for postnatal TEC survival. Furthermore, we found no evidence of selective effects of MCL-1 deletion on CD45⁺EpCAM⁺ non-epithelial stroma (**Figure 6D right**), suggesting that the specific loss of TEC we observed following *Mcl1* deletion reflects an ongoing requirement for this pro-survival protein in TEC homeostasis.

EGF Regulates MCL-1 Expression in TECs

The present data suggest that the mechanisms that regulate MCL-1 expression in TEC are pertinent to thymic function. Since reciprocal interactions between thymocytes and TEC (termed “thymic crosstalk”) constitute an important axis for

TEC development, we first addressed whether thymocytes affect MCL-1 expression by TECs. Thymic lobes from E15.5 mice were cultured for 5 days in FTOC with 2'-deoxyguanosine (2-Guo) to selectively deplete thymocytes. We found that the depletion of thymocytes did not influence MCL-1 levels in TECs, as measured by intracellular flow cytometry (**Figure 7A**). We also tested three prominent thymocyte-derived TEC growth factors, CD40L, RANKL or IL-22 as regulators of MCL-1 expression^{39,40}, but none of these ligands altered MCL-1 levels in TEC in 2-dGuo cultured thymic lobes (**Figure 7B**), consistent with the observation that the loss of thymocytes does not alter the levels of MCL-1 protein in TECs.

To identify signals derived from non-haematopoietic cells that regulate MCL-1 levels in TECs, we tested factors that have been demonstrated to support TEC survival, including epidermal growth factor (EGF)⁴¹, fibroblast growth factor 10 (FGF-10)⁴² and hepatocyte growth factor (HGF)⁴³ (**Figure 7C**). Using the same assay, we found that EGF substantially augmented the levels of MCL-1 in all TECs (**Figure 7C**). To determine the pathway mediating this activity, we employed well-characterized inhibitors of EGFR signaling^{44,45}. EGF-mediated MCL-1 upregulation in TEC was completely prevented by the MAPK/ERK kinase (MEK) inhibitors U0126, PD98059 and PD0325901⁴⁵ (**Figure 7D**). These data show that EGF regulates expression of pro-survival MCL-1 in TEC via the MAPK/ERK pathway, consistent with the importance of EGF for supporting thymus development^{41,43-45}.

Discussion

Our findings reveal several important aspects of the molecular control of TEC survival. Surprisingly, despite substantial expression of BCL-2 and BCL-XL, these pro-survival proteins appear largely dispensable for TEC homeostasis and thymic function. Whether there might be distinct requirements for these pro-survival proteins in thymic protection or recovery from insults, such as chemotherapy or viral infection, warrants further investigation. By contrast, steady-state thymic function relies upon MCL-1 expression by TEC. Among the pro-survival BCL-2 family members, MCL-1 is distinguished by strict post-translational regulatory mechanisms, a high protein turnover and a critical role in the survival of multiple haematopoietic lineages⁴⁶. However, MCL-1 is by no means a “universal” survival protein. It is dispensable for the survival of megakaryocytes, platelets⁴⁷, monocytes, macrophages^{48,49}, pre-pubertal mammary epithelium²⁶. Moreover, the distinct regulation of MCL-1 expression in haematopoietic cells (mediated by common- γ chain cytokines) and TECs (mediated, at least in part, by EGF) highlight tissue-specific mechanisms that govern the homeostasis of these lineages.

A feature of the thymic defects in *Mcl1* ^{Δ Foxn1} mice was that they became severe only sometime after the perinatal stages. Although the thymus size decreased in E15.5 and day 9 *Mcl1* ^{Δ Foxn1} mice, all of the major TEC subtypes were present and capable of supporting reduced thymocyte differentiation, indicating that TEC differentiation remains intact in *Mcl1* ^{Δ Foxn1} mice. Yet, their survival was not supported as the thymus matured and mTEC were particularly reliant upon MCL-1, since this compartment was substantially diminished by day 9 and essentially absent by 2 months of age. In the cortex, the increased proportion of cycling $\beta 5t^+$, K5/K8⁺, DEC205⁻ and CD40⁺ cTEC and impaired production of key thymocyte growth factors

indicated the loss of mature cTEC in *Mcl1* ^{Δ Foxn1} mice could be driving the loss of early thymocyte subsets. All of these features were completely rescued by deletion of the pro-apoptotic effector protein, BAK, demonstrating that MCL-1 is essential for preventing the premature apoptosis of these mature TEC.

Why is there a delay in thymic atrophy following loss of MCL-1 in TEC? It is notable that the timing of medullary collapse and thymic atrophy in *Mcl1* ^{Δ Foxn1} mice corresponds with an apparent switch in the origin of mTECs. TEC progenitors with a cortical phenotype give rise to a substantial proportion of mTEC early in life; however, this contribution ceases after 1-2 weeks and mTEC-restricted cells maintain the mature medullary compartment⁵⁰. Further investigation of this temporal window in *Mcl1* ^{Δ Foxn1} mice may yield insights into how progenitor cells respond to perturbation of TEC homeostasis caused by loss of differentiated mTEC. For instance, the increased TEC proliferation observed at E15.5 and day 9 is consistent with the notion that elevated bipotent progenitor activity in the cTEC compartment can initially compensate for mature TEC loss in *Mcl1* ^{Δ Foxn1} mice but is unable to maintain this role into adulthood.

Another question raised by these data is whether MCL-1 might drive age-related thymic involution. We could find no significant difference in MCL-1 expression in TEC from 2 month-old versus 1 year-old mice (data not shown), suggesting that this is not the case.

The critical role for MCL-1 in TEC survival raises the question of how the thymic microenvironment regulates this BCL-2 family member in TEC. Among a range of TEC trophic cytokines tested, only EGF positively regulated MCL-1 expression in TEC from 2-dGuo FTOC. Interestingly, TEC expression of EGFR is required for proper mTEC number and architecture⁴³; however, the extent of these

defects is milder than those we observe here, suggesting that there are other regulators of MCL-1 in TEC. In light of these findings, it will be of interest to determine the best strategies for inducing MCL-1 upregulation to support TEC survival in age- or insult-induced thymic atrophy.

The impaired function of the immune system in aged individuals and patients that are unable to restore immune function following thymic insult induced by cancer treatments or infections leads to substantial morbidity and mortality due to higher rates of opportunistic infections, cancer and autoimmunity⁵¹⁻⁵⁴. Several studies have reported stimulating TEC growth represents a compelling strategy to rejuvenate thymic function in clinical settings⁵⁵⁻⁵⁷. Partial regeneration was observed in mice administered with keratinocyte growth factor (KGF) via the induction of TEC proliferation^{55,58,59}. The combined administration of KGF and an inhibitor of p53, PFT- β , accelerated thymic recovery by restoring TEC numbers after bone marrow transplantation⁵⁶. Our findings indicate that MCL-1 expression is an important biomarker of TEC survival in these contexts. Furthermore, co-administration of factors that target distinct cellular processes in TEC (i.e. proliferation and MCL-1-mediated survival) may promote more robust and durable thymic regeneration than has been observed to-date.

Acknowledgements

We gratefully acknowledge the Gray, Strasser and Herold labs for valuable feedback. We thank the WEHI Flow Cytometry Laboratory and the Centre for Dynamic Imaging, for technical assistance; B Helbert, K Mackwell, C Young for mouse genotyping; G Siciliano, K Humphreys, S O'Connor and H Marks for animal husbandry and S Wilcox, N Lalaoui, D Vremec, R Boyd, A Chidgey, P Bouillet, S Grabow, G Kelly, B Kile and I Tabas and L Hennighausen for animals, technical assistance and/or reagents. TROMA-I was deposited to the DSHB by Brulet, and Kemler (DSHB Hybridoma Product TROMA-I). This work was supported by grants GNT0637353, GNT1049724 and GNT1121325 and Career Development Fellowship-2 1090236 (for D.H.D.G.), 1016701, Senior Principal Research Fellow [SPRF] Fellowship 1020363 (for A.S), Australia Fellowship (for J.V.), GNT1086727 (for N.F), GNT 1054618 (for G.K.S), 1058892 (for L.G) from the Australian National Health and Medical Research Council, Wellcome Trust 105045/Z/14/Z (for G.H), the Leukemia & Lymphoma Society of America (Specialized Center of Research [SCOR] grant. 7001-13), the Leukaemia Research Foundation and MIRS and MIFRS (for R.J.) from the University of Melbourne. This work was made possible through Victorian State Government Operational Infrastructure Support and Australian Government NHMRC IRIISS.

Author Contributions

Conceptualization, R.J., A.S. and D.H.D.G.; Methodology, R.J., J.M.S., A.S. and D.H.D.G.; Investigation, R.J., J.M.S., A.P., M.H., G.K.S, L.G., G.D., S.S., and D.H.D.G.; Resources, S.S., N.Y.F., J.E.V., G.H., A.S., D.H.D.G.; Writing - Original draft, R.J., J.M.S., and D.H.D.G.; Writing – Review and editing, R.J., J.M.S., G.H., A.S. and D.H.D.G.

Disclosure of Conflicts of Interest

The authors declare no conflict of interest. Correspondence and requests for materials should be addressed to D.H.D.G. (dgray@wehi.edu.au).

References

1. Ohigashi I, Kozai M, Takahama Y. Development and developmental potential of cortical thymic epithelial cells. *Immunol Rev.* 2016;271(1):10-22.
2. Perry JS, Hsieh CS. Development of T-cell tolerance utilizes both cell-autonomous and cooperative presentation of self-antigen. *Immunol Rev.* 2016;271(1):141-155.
3. Irla M, Hollander G, Reith W. Control of central self-tolerance induction by autoreactive CD4⁺ thymocytes. *Trends Immunol.* 2010;31(2):71-79.
4. Boehm T, Swann JB. Thymus involution and regeneration: two sides of the same coin? *Nat Rev Immunol.* 2013;13(11):831-838.
5. Chaudhry MS, Velardi E, Dudakov JA, van den Brink MR. Thymus: the next (re)generation. *Immunol Rev.* 2016;271(1):56-71.
6. Dumont-Lagace M, Brochu S, St-Pierre C, Perreault C. Adult thymic epithelium contains non-senescent label-retaining cells. *J Immunol.* 2014;192(5):2219-2226.
7. Gabler J, Arnold J, Kyewski B. Promiscuous gene expression and the developmental dynamics of medullary thymic epithelial cells. *Eur J Immunol.* 2007;37(12):3363-3372.

8. Gray D, Abramson J, Benoist C, Mathis D. Proliferative arrest and rapid turnover of thymic epithelial cells expressing Aire. *J Exp Med*. 2007;204(11):2521-2528.
9. Gray DH, Seach N, Ueno T, et al. Developmental kinetics, turnover, and stimulatory capacity of thymic epithelial cells. *Blood*. 2006;108(12):3777-3785.
10. Rossi SW, Kim MY, Leibbrandt A, et al. RANK signals from CD4(+)3(-) inducer cells regulate development of Aire-expressing epithelial cells in the thymic medulla. *J Exp Med*. 2007;204(6):1267-1272.
11. Colome N, Collado J, Bech-Serra JJ, et al. Increased apoptosis after autoimmune regulator expression in epithelial cells revealed by a combined quantitative proteomics approach. *J Proteome Res*. 2010;9(5):2600-2609.
12. Liiv I, Haljasorg U, Kisand K, Maslovskaja J, Laan M, Peterson P. AIRE-induced apoptosis is associated with nuclear translocation of stress sensor protein GAPDH. *Biochem Biophys Res Commun*. 2012;423(1):32-37.
13. Metzger TC, Khan IS, Gardner JM, et al. Lineage tracing and cell ablation identify a post-Aire-expressing thymic epithelial cell population. *Cell Rep*. 2013;5(1):166-179.
14. Nishikawa Y, Nishijima H, Matsumoto M, et al. Temporal lineage tracing of Aire-expressing cells reveals a requirement for Aire in their maturation program. *J Immunol*. 2014;192(6):2585-2592.

15. Adams JM, Cory S. The Bcl-2 apoptotic switch in cancer development and therapy. *Oncogene*. 2007;26(9):1324-1337.
16. Wang YH, Scadden DT. Harnessing the apoptotic programs in cancer stem-like cells. *EMBO Rep*. 2015;16(9):1084-1098.
17. Anderson MA, Huang D, Roberts A. Targeting BCL2 for the treatment of lymphoid malignancies. *Semin Hematol*. 2014;51(3):219-227.
18. Vikstrom I, Carotta S, Luthje K, et al. Mcl-1 is essential for germinal center formation and B cell memory. *Science*. 2010;330(6007):1095-1099.
19. Wagner KU, Claudio E, Rucker EB, 3rd, et al. Conditional deletion of the Bcl-x gene from erythroid cells results in hemolytic anemia and profound splenomegaly. *Development*. 2000;127(22):4949-4958.
20. Thorp E, Li Y, Bao L, et al. Brief report: increased apoptosis in advanced atherosclerotic lesions of Apoe^{-/-} mice lacking macrophage Bcl-2. *Arterioscler Thromb Vasc Biol*. 2009;29(2):169-172.
21. Grabow S, Delbridge AR, Valente LJ, Strasser A. MCL-1 but not BCL-XL is critical for the development and sustained expansion of thymic lymphoma in p53-deficient mice. *Blood*. 2014;124(26):3939-3946.
22. Zuklys S, Gill J, Keller MP, et al. Stabilized beta-catenin in thymic epithelial cells blocks thymus development and function. *J Immunol*. 2009;182(5):2997-3007.

23. Lindsten T, Ross AJ, King A, et al. The combined functions of proapoptotic Bcl-2 family members bak and bax are essential for normal development of multiple tissues. *Mol Cell*. 2000;6(6):1389-1399.
24. Caton ML, Smith-Raska MR, Reizis B. Notch-RBP-J signaling controls the homeostasis of CD8- dendritic cells in the spleen. *J Exp Med*. 2007;204(7):1653-1664.
25. Sansom SN, Shikama-Dorn N, Zhanybekova S, et al. Population and single-cell genomics reveal the Aire dependency, relief from Polycomb silencing, and distribution of self-antigen expression in thymic epithelia. *Genome Res*. 2014;24(12):1918-1931.
26. Fu NY, Rios AC, Pal B, et al. EGF-mediated induction of Mcl-1 at the switch to lactation is essential for alveolar cell survival. *Nat Cell Biol*. 2015;17(4):365-375.
27. Jain R, Gray DH. Isolation of thymic epithelial cells and analysis by flow cytometry. *Curr Protoc Immunol*. 2014;107:3 26 21-15.
28. Okamoto T, Coultas L, Metcalf D, et al. Enhanced stability of Mcl1, a prosurvival Bcl2 relative, blunts stress-induced apoptosis, causes male sterility, and promotes tumorigenesis. *Proc Natl Acad Sci U S A*. 2014;111(1):261-266.
29. Allan C, Burel JM, Moore J, et al. OMERO: flexible, model-driven data management for experimental biology. *Nat Methods*. 2012;9(3):245-253.

30. Kim D, Langmead B, Salzberg SL. HISAT: a fast spliced aligner with low memory requirements. *Nat Methods*. 2015;12(4):357-360.
31. Trapnell C, Roberts A, Goff L, et al. Differential gene and transcript expression analysis of RNA-seq experiments with TopHat and Cufflinks. *Nat Protoc*. 2012;7(3):562-578.
32. de Jonge HJ, Fehrman RS, de Bont ES, et al. Evidence based selection of housekeeping genes. *PLoS One*. 2007;2(9):e898.
33. Almeida AR, Borghans JA, Freitas AA. T cell homeostasis: thymus regeneration and peripheral T cell restoration in mice with a reduced fraction of competent precursors. *J Exp Med*. 2001;194(5):591-599.
34. Prockop SE, Petrie HT. Regulation of thymus size by competition for stromal niches among early T cell progenitors. *J Immunol*. 2004;173(3):1604-1611.
35. Cowan JE, Parnell SM, Nakamura K, et al. The thymic medulla is required for Foxp3⁺ regulatory but not conventional CD4⁺ thymocyte development. *J Exp Med*. 2013;210(4):675-681.
36. den Braber I, Mugwagwa T, Vrisekoop N, et al. Maintenance of peripheral naive T cells is sustained by thymus output in mice but not humans. *Immunity*. 2012;36(2):288-297.

37. Klug DB, Carter C, Crouch E, Roop D, Conti CJ, Richie ER. Interdependence of cortical thymic epithelial cell differentiation and T-lineage commitment. *Proc Natl Acad Sci U S A*. 1998;95(20):11822-11827.
38. Tarutani M, Itami S, Okabe M, et al. Tissue-specific knockout of the mouse *Pig-a* gene reveals important roles for GPI-anchored proteins in skin development. *Proc Natl Acad Sci U S A*. 1997;94(14):7400-7405.
39. Akiyama T, Shimo Y, Yanai H, et al. The tumor necrosis factor family receptors RANK and CD40 cooperatively establish the thymic medullary microenvironment and self-tolerance. *Immunity*. 2008;29(3):423-437.
40. Dudakov JA, Hanash AM, Jenq RR, et al. Interleukin-22 drives endogenous thymic regeneration in mice. *Science*. 2012;336(6077):91-95.
41. Shinohara T, Honjo T. Epidermal growth factor can replace thymic mesenchyme in induction of embryonic thymus morphogenesis in vitro. *Eur J Immunol*. 1996;26(4):747-752.
42. Revest JM, Suniara RK, Kerr K, Owen JJ, Dickson C. Development of the thymus requires signaling through the fibroblast growth factor receptor R2-IIIb. *J Immunol*. 2001;167(4):1954-1961.
43. Satoh R, Kakugawa K, Yasuda T, et al. Requirement of Stat3 Signaling in the Postnatal Development of Thymic Medullary Epithelial Cells. *PLoS Genet*. 2016;12(1):e1005776.

44. Chandra A, Lan S, Zhu J, Siclari VA, Qin L. Epidermal growth factor receptor (EGFR) signaling promotes proliferation and survival in osteoprogenitors by increasing early growth response 2 (EGR2) expression. *J Biol Chem*. 2013;288(28):20488-20498.
45. Leu CM, Chang C, Hu C. Epidermal growth factor (EGF) suppresses staurosporine-induced apoptosis by inducing mcl-1 via the mitogen-activated protein kinase pathway. *Oncogene*. 2000;19(13):1665-1675.
46. Opferman JT. Life and death during hematopoietic differentiation. *Curr Opin Immunol*. 2007;19(5):497-502.
47. Debrincat MA, Josefsson EC, James C, et al. Mcl-1 and Bcl-x(L) coordinately regulate megakaryocyte survival. *Blood*. 2012;119(24):5850-5858.
48. Dzhagalov I, St John A, He YW. The antiapoptotic protein Mcl-1 is essential for the survival of neutrophils but not macrophages. *Blood*. 2007;109(4):1620-1626.
49. Steimer DA, Boyd K, Takeuchi O, Fisher JK, Zambetti GP, Opferman JT. Selective roles for antiapoptotic MCL-1 during granulocyte development and macrophage effector function. *Blood*. 2009;113(12):2805-2815.
50. Ohigashi I, Zuklys S, Sakata M, et al. Adult Thymic Medullary Epithelium Is Maintained and Regenerated by Lineage-Restricted Cells Rather Than Bipotent Progenitors. *Cell Rep*. 2015;13(7):1432-1443.

51. Day CL, Kaufmann DE, Kiepiela P, et al. PD-1 expression on HIV-specific T cells is associated with T-cell exhaustion and disease progression. *Nature*. 2006;443(7109):350-354.
52. Douek DC, McFarland RD, Keiser PH, et al. Changes in thymic function with age and during the treatment of HIV infection. *Nature*. 1998;396(6712):690-695.
53. Douek DC, Vescio RA, Betts MR, et al. Assessment of thymic output in adults after haematopoietic stem-cell transplantation and prediction of T-cell reconstitution. *Lancet*. 2000;355(9218):1875-1881.
54. Storek J, Gooley T, Witherspoon RP, Sullivan KM, Storb R. Infectious morbidity in long-term survivors of allogeneic marrow transplantation is associated with low CD4 T cell counts. *Am J Hematol*. 1997;54(2):131-138.
55. Alpdogan O, Hubbard VM, Smith OM, et al. Keratinocyte growth factor (KGF) is required for postnatal thymic regeneration. *Blood*. 2006;107(6):2453-2460.
56. Kelly RM, Goren EM, Taylor PA, et al. Short-term inhibition of p53 combined with keratinocyte growth factor improves thymic epithelial cell recovery and enhances T-cell reconstitution after murine bone marrow transplantation. *Blood*. 2010;115(5):1088-1097.
57. Kelly RM, Highfill SL, Panoskaltsis-Mortari A, et al. Keratinocyte growth factor and androgen blockade work in concert to protect against conditioning

regimen-induced thymic epithelial damage and enhance T-cell reconstitution after murine bone marrow transplantation. *Blood*. 2008;111(12):5734-5744.

58. Erickson M, Morkowski S, Lehar S, et al. Regulation of thymic epithelium by keratinocyte growth factor. *Blood*. 2002;100(9):3269-3278.

59. Rossi SW, Jeker LT, Ueno T, et al. Keratinocyte growth factor (KGF) enhances postnatal T-cell development via enhancements in proliferation and function of thymic epithelial cells. *Blood*. 2007;109(9):3803-3811.

Figure legends

Figure 1. Loss of MCL-1 in TEC precipitates thymic hypoplasia.

(A) Heat-map of BCL-2 family member expression in the indicated TEC subsets from 1 week- or 4 week-old WT or *Aire*^{-/-} mice as assessed by RNA sequencing (n=2). TEC subsets and genes are hierarchically clustered by Pearson correlation and Euclidean distance, respectively. Genes encoding pro-survival proteins are highlighted in blue. (B) Histograms of flow cytometric analysis of BCL-2 (**top**), BCL-XL (**middle**) and MCL-1 levels (**bottom**) in TEC subsets from 2 month-old WT mice. (C) Histograms of flow cytometric analysis of BCL-2 (**top**), BCL-XL (**middle**) and MCL-1 (**bottom**) expression in CD45⁻EpCAM⁺MHCII⁺ TECs isolated from day 9, 1 month and E15.5 embryos, respectively, of the indicated genotypes. (D) Pictures of thymi from 2 month-old female mice of the indicated genotypes. (E) Thymic cellularity of 2 month-old mice of the indicated genotypes. (F) Thymic cellularity of controls (black circles) and *Mcl1*^{ΔFoxn1} (grey squares) mice at various ages. The numbers in parentheses indicate the mean fold change in thymic cellularity (controls/*Mcl1*^{ΔFoxn1} mice). Data representative of at least two independent experiments are shown. Graph bars indicate mean ± SEM and groups were compared with a Student's t test (two sided, unpaired). * p<0.05; ** p<0.01; *** p<0.001; **** p<0.0001. The control group includes various combinations of genotypes (*Foxn1*^{Cre/+}*Mcl1*^{+/+}, *Foxn1*^{+/+}*Mcl1*^{lox/+}, *Foxn1*^{+/+}*Mcl1*^{lox/lox}, *Foxn1*^{Cre/+}*Mcl1*^{lox/+}) that showed no differences from each other in separate experiments (n≥3/group).

Figure 2. Reduced thymocytes and thymic Foxp3⁺ regulatory T cells in *Mcl1*^{ΔFoxn1} mice.

(A) Flow cytometry plots of CD4 vs. CD8 expression on thymocytes. Graphs represent the numbers of different thymocyte and DN subsets in the thymus. (B) Flow cytometry plots of CD4 vs. FOXP3 gated on CD4SP thymocytes, with the proportion of cell bounded by regions indicated. Graphs show the proportion and number of thymic FOXP3⁺ Treg cells from controls and *Mcll*^{ΔFoxn1} mice at the indicated ages. Data representative of at least two independent experiments are shown (except Treg cell data for 2 months). Graph bars indicate mean ± SEM and groups were compared with a Student's t test (two sided, unpaired). ** p<0.01; *** p<0.001; **** p<0.0001. The control group combines various combinations of genotypes (*Foxn1*^{Cre/+}*Mcll*^{+/+}, *Foxn1*^{+/+}*Mcll*^{lox/+}, *Foxn1*^{+/+}*Mcll*^{lox/lox}, *Foxn1*^{Cre/+}*Mcll*^{lox/+}) that showed no differences from each other in separate experiments (n ≥ 3/group; where n represents the number of mice per group with each point denoting a mouse).

Figure 3. Deficiency in peripheral naïve T cells in *Mcll*^{ΔFoxn1} mice.

(A) Graphs show the numbers of CD4⁺ and CD8⁺ T cells gated on splenic TCRβ⁺. (B, C) Flow cytometry plots of CD44 vs. CD62L gated on splenic TCRβ⁺CD4⁺ (B) or TCRβ⁺CD8⁺ (C) T cells. Graphs show the numbers of naïve (CD44^{low}/CD62L^{high}), effector (CD44^{high}/CD62L^{low}) and central memory (CD44^{high}/CD62L^{high}) TCRβ⁺CD4⁺ (B) or CD8⁺ (C) from controls and *Mcll*^{ΔFoxn1} mice. (D) Graphs show the proportions of proliferating (Ki67⁺) CD4⁺ and CD8⁺ T cells from controls and *Mcll*^{ΔFoxn1} mice at indicated ages. (E) Graphs show the proportions of splenic Treg cells from controls and *Mcll*^{ΔFoxn1} mice at the indicated time points. Graph bars indicate mean ± SEM and groups were compared with a Student's t test (two sided, unpaired). * p<0.05; ** p<0.01; *** p<0.001; **** p<0.0001. Controls include various combinations of genotypes (*Foxn1*^{Cre/+}*Mcll*^{+/+}, *Foxn1*^{+/+}*Mcll*^{lox/+}, *Foxn1*^{+/+}*Mcll*^{lox/lox},

Foxn1^{Cre/+}*Mcl1*^{lox/+}) that showed no differences from each other in separate experiments (n ≥ 3/group).

Figure 4. Progressive loss of TEC in *Mcl1*^{ΔFoxn1} mice.

(A) TEC (CD45⁺MHCII⁺EpCAM⁺) numbers from control and *Mcl1*^{ΔFoxn1} mice at different time points. (B-D) Representative flow cytometry plots (B) and graphs showing proportions (C) and absolute numbers (D) of cTECs (Ly51⁺UEA-1⁻) and CD80⁺ and CD80⁻ mTECs or total mTECs (Ly51⁻UEA-1⁺). (E, F) Representative flow cytometry plots (E) and graphs showing absolute numbers (F) of CD80⁺ mTECs expressing AIRE in day 9 *Mcl1*^{ΔFoxn1} mice. (G) Representative histograms (black and grey histograms show controls and *Mcl1*^{ΔFoxn1} mice, respectively) and (H) graphs showing proportions of proliferating Ki67⁺ TECs. Data are representative of at least two independent experiments (n ≥ 3/group) (except TEC subset data for day 9). Graph bars indicate mean ± SEM and groups were compared with a Student's t test (two sided, unpaired). * p<0.05; ** p<0.01; *** p<0.001; **** p<0.0001. The control group combines various combinations of genotypes (*Foxn1*^{Cre/+}*Mcl1*^{+/+}, *Foxn1*^{+/+}*Mcl1*^{lox/+}, *Foxn1*^{+/+}*Mcl1*^{lox/lox}, *Foxn1*^{Cre/+}*Mcl1*^{lox/+}) that showed no differences from each other in separate experiments. (I-L) Immunofluorescence images of thymic sections from day 9 and 2 month-old control and *Mcl1*^{ΔFoxn1} mice stained with anti-K8, anti-K5 and UEA-1 (I), anti-DEC205 and anti-PanK (J), anti-PanK and AIRE (K) and ER-TR7 and anti-PanK (L). Scale bars represent 100 μm (I, J, L) and 50 μm (K).

Figure 5. MCL-1 is required for mature TEC survival

(A) Multi dimension scaling (MDS) plot comparing RNA-seq expression profiles for cTECs and mTECs from one month old controls and *Mcll* ^{Δ Foxn1} mice. Libraries are labelled and coloured according to the genotype and TEC subset. Distances on the plot correspond to leading log2-fold-change between each pair of samples. (B) Genes that were differentially expressed (FDR<0.05) in *Mcll* ^{Δ Foxn1} cTEC relative to controls that are involved in TEC (black) or thymocyte (grey) development. (C-F) Histograms of β 5t (C), CD40 (D) expression in CD45⁻EpCAM⁺MHCII⁺Ly51⁺ cTECs and MHCII (E), CD80 (F) in CD45⁻EpCAM⁺MHCII⁺ TECs isolated from 5 weeks old mice (blue and red histograms show controls and *Mcll* ^{Δ Foxn1} mice, respectively). (G) Thymic cellularity (left) and TEC (CD45⁻MHCII⁺EpCAM⁺) numbers (right) of 4-7 week-old mice of the indicated genotypes. (H) Histogram of flow cytometric analysis of MCL-1 expression in CD45⁻EpCAM⁺MHCII⁺ TECs isolated from 4-7 week-old mice of the indicated genotypes. Data are representative of three independent experiments (n \geq 2/group) (except A-F). Graph bars indicate mean \pm SEM and groups were compared with a Student's t test (two sided, unpaired). ** p<0.01; *** p<0.001; **** p<0.0001.

Figure 6. An ongoing requirement for MCL-1 in TEC survival.

(A) Representative flow cytometry plots of MCL-1 expression in CD45⁻EpCAM⁺MHCII⁺ TEC isolated from grafts 5 days after the third dose of tamoxifen treatment. (B) Photos of experimental (denoted as “E” for *Rosa*^{CreERT2} *Mcll*^{lox/lox}) and control (“C”) thymic lobes grafted under the renal capsule of C57BL/6-Ly5.1 males analysed at indicated time points after three doses of tamoxifen treatment. (C) Total cell numbers recovered from grafts at the indicated time points after third dose of tamoxifen treatment. (D) Flow cytometry plots of MHCII and EpCAM gated on CD45⁻EpCAM⁺ TEC (representative of ~~four~~ three experiments performed on 14-17

mice) and graphs of the number of CD45⁻EpCAM⁺MHCII⁺ TEC (middle) and proportion of CD45⁻EpCAM⁺ recovered from grafts 5 days after the third dose of tamoxifen treatment. Bars indicate mean \pm SEM and groups were compared with a Student's t test (two sided, unpaired). *** p<0.001; ****p<0.0001. Controls include various combinations of genotypes (*Rosa*^{Cre/Cre}*MclI*^{lox/+}, *Rosa*^{+/+}*MclI*^{lox/+}, *Rosa*^{+/+}*MclI*^{lox/lox}).

Figure 7. EGF regulates MCL-1 expression in TEC.

(A) Histogram of MCL-1 expression in CD45⁻EpCAM⁺MHCII⁺ TEC from FTOC with or without 2-dGuo treatment. (B-D) Histograms of MCL-1 expression in CD45⁻EpCAM⁺ MHCII⁺ TEC from 2-dGuo-FTOC left untreated (**blue**) or stimulated (**red**) with RANKL, agonist CD40 antibody, IL-22 (**B**), FGF-10, HGF, EGF (**C**), EGF+U0126, EGF+PD98059 and EGF+PD0325901 (**D**). Data are representative of at least two experiments with n=3/treatment. Numbers in **D** plots indicate the geometric mean of the fluorescence intensity.

Figure 1

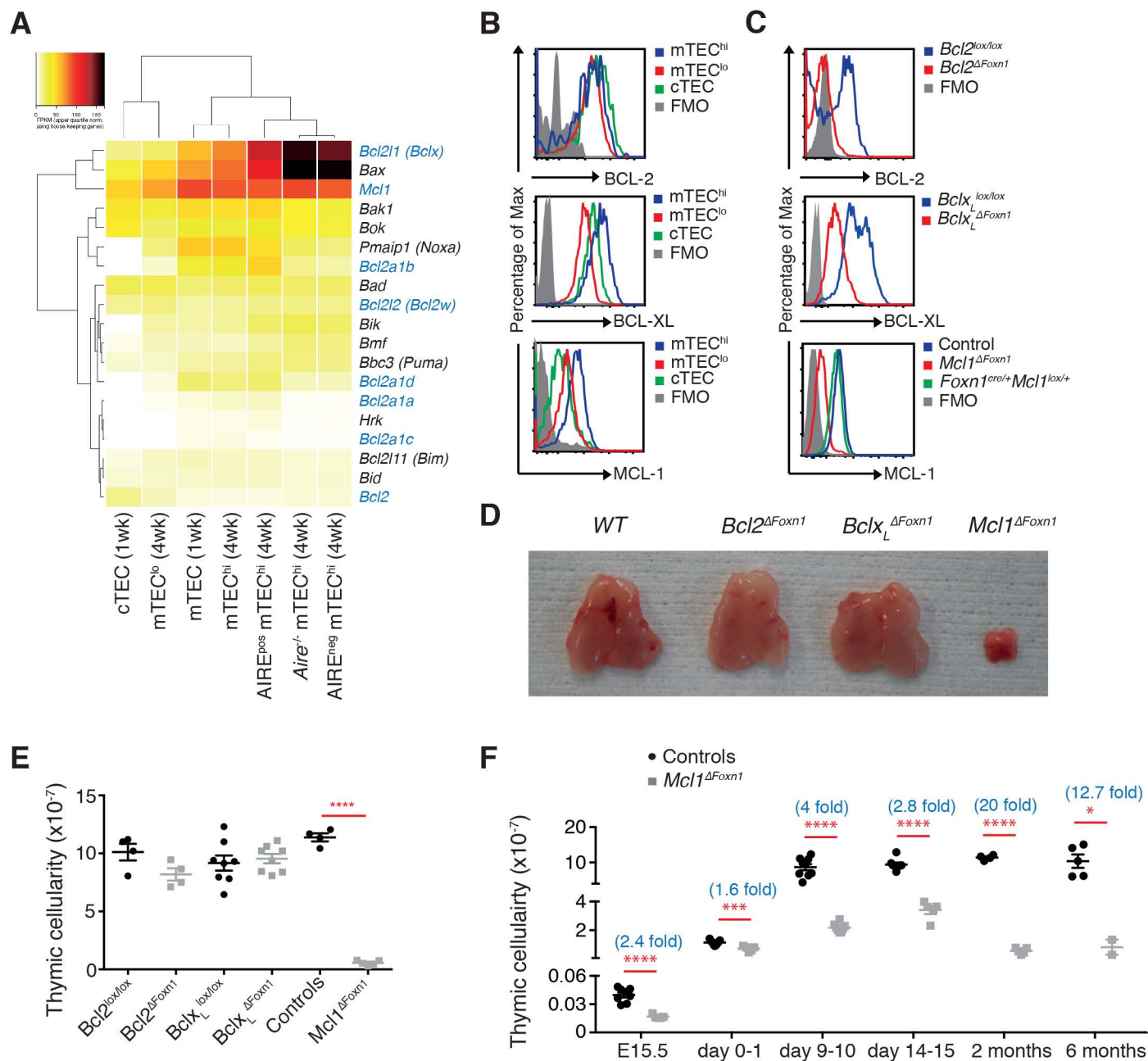


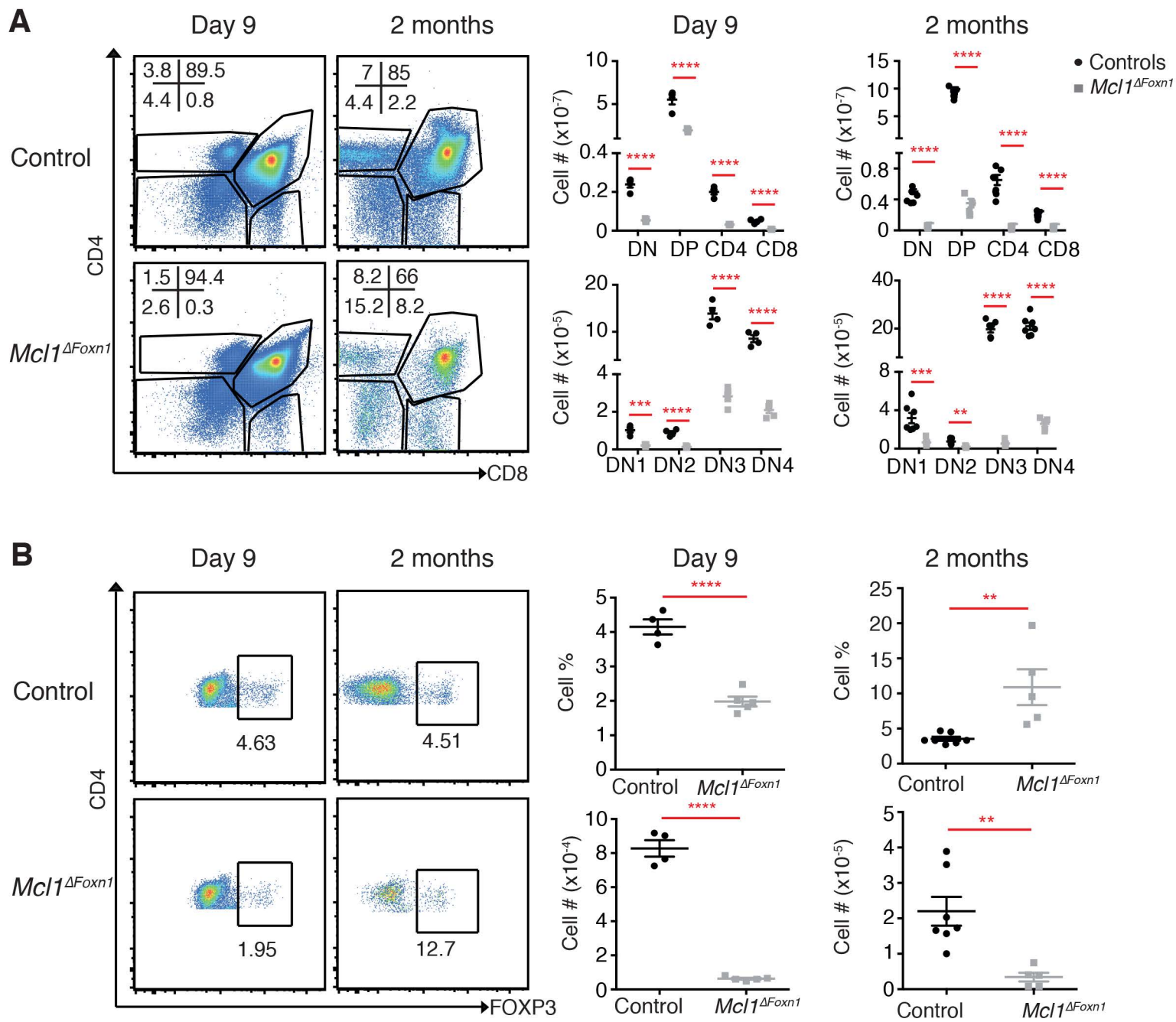
Figure 2

Figure 3

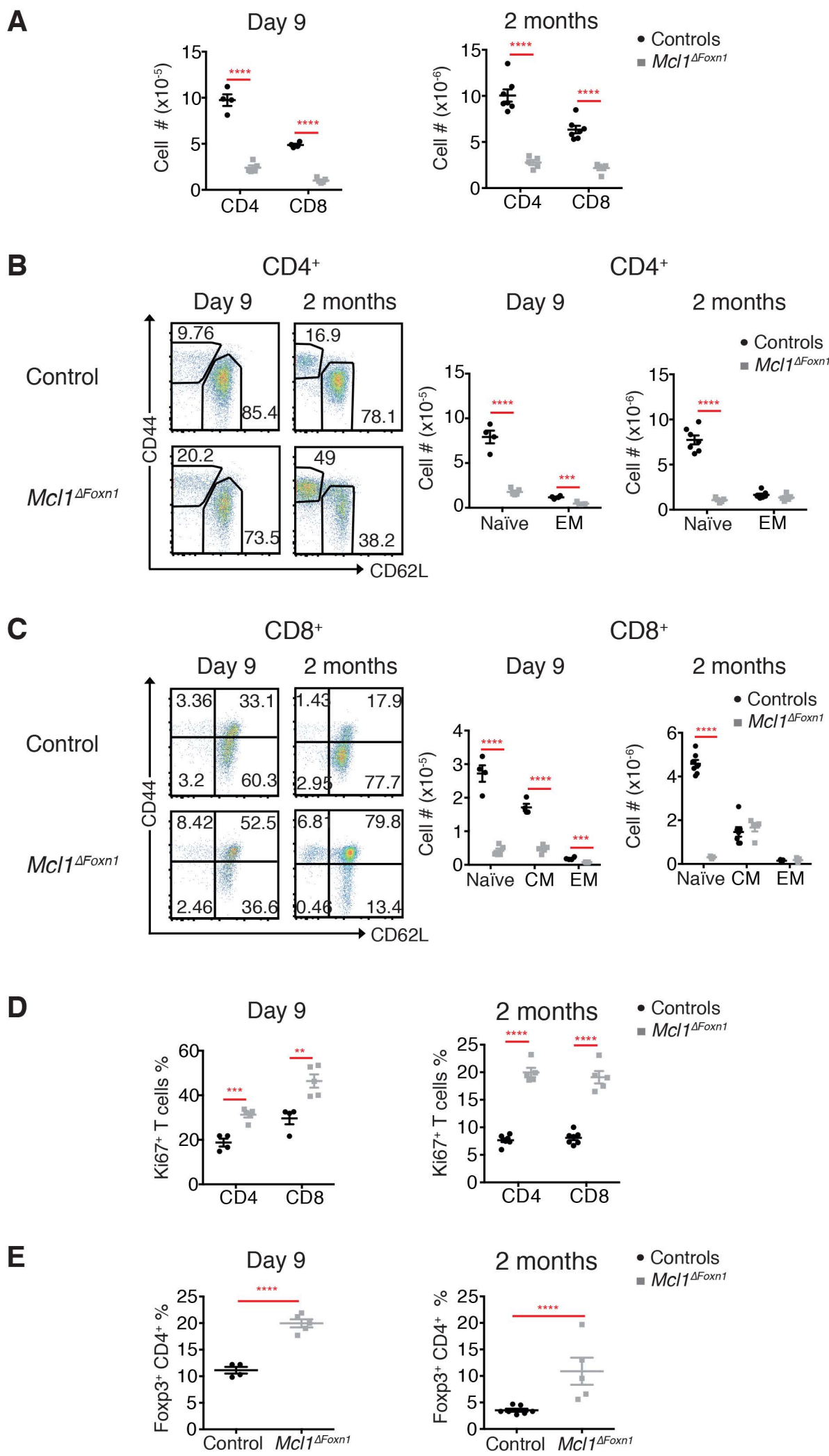


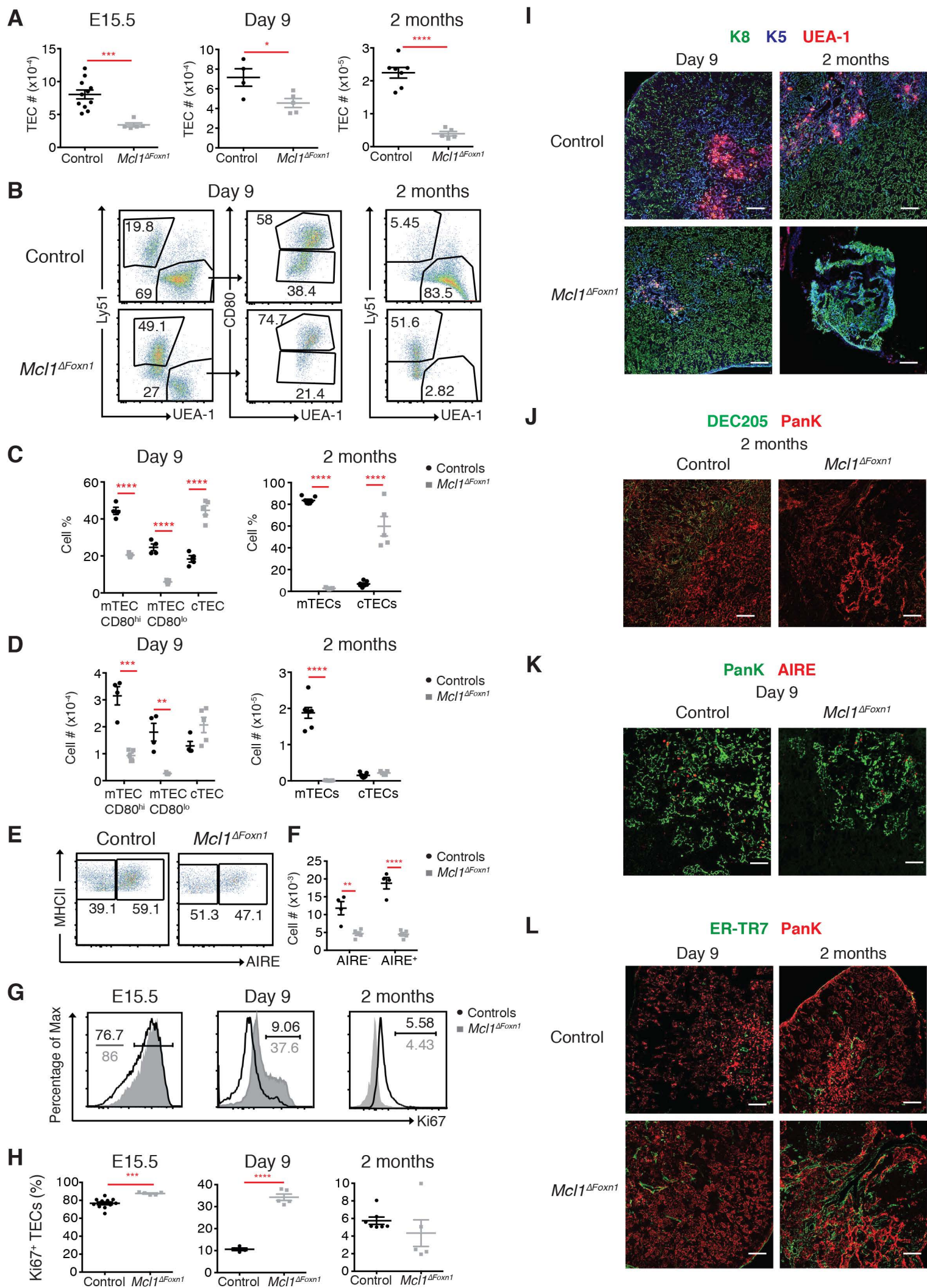
Figure 4

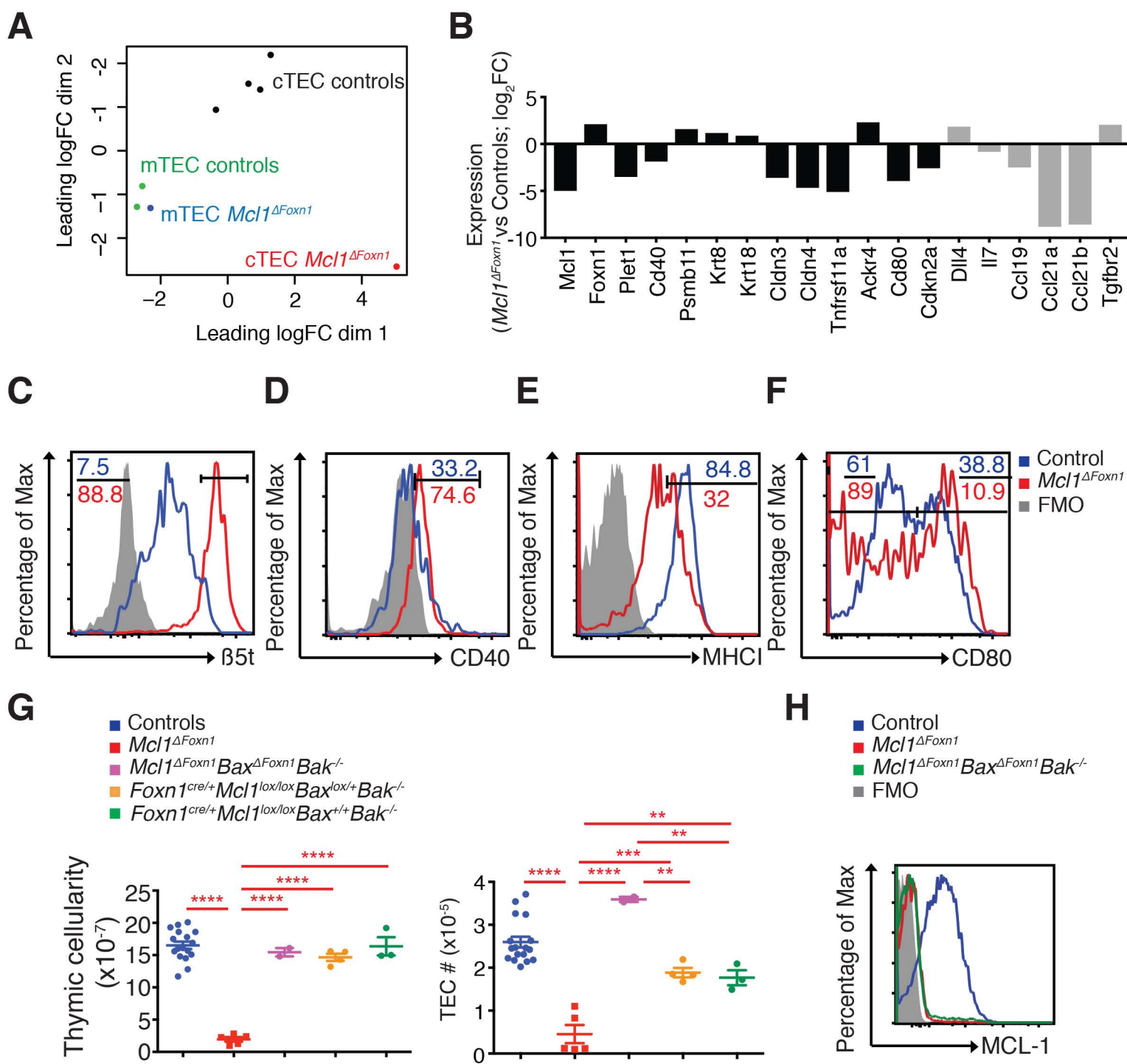
Figure 5

Figure 6

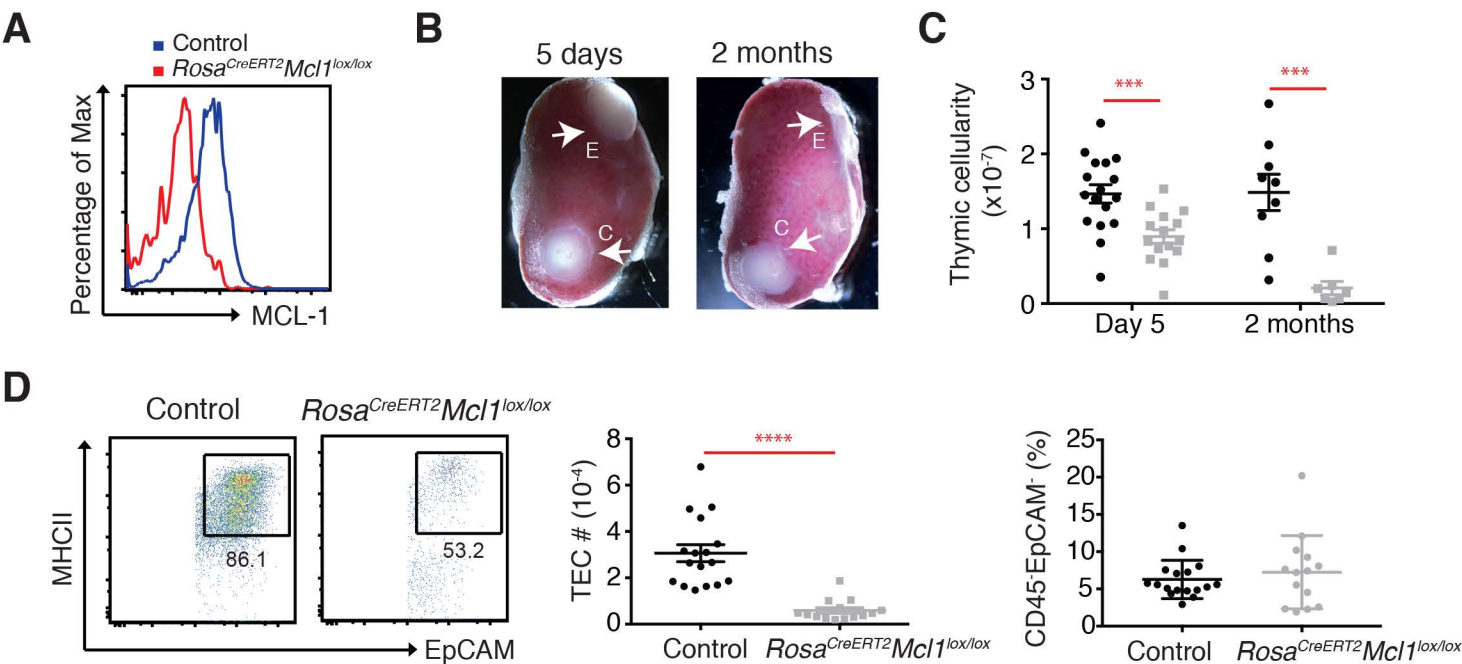


Figure 7

